EVALUATION OF STRUCTURAL PERFORMANCE BASED ON AN ENERGY BALANCE APPROACH

K.K.F. Wong[1], S.L. McCabe[2]

[1] *Research Structural Engineer, National Institute of Standards and Technology, kevin.wong@nist.gov*
[2] *Group Leader, National Institute of Standards and Technology, steven.mccabe@nist.gov*

Abstract

An analytical method is developed to quantify the potential energy and other energy characteristics of the nonlinear response of framed structures subjected to earthquake ground motions. Since the potential energy relates to the stiffness of the structure, it consists of three components in a nonlinear system: (1) stored strain energy associated with the linear elastic portion of the structural response, which can be recovered after the earthquake; (2) higher-order energy associated with geometric nonlinear behavior of the structural response, which is derived from the nonlinear stiffness matrix and can also be recovered if the axial load is removed; and (3) plastic energy representing the energy dissipated by inelastic deformation of the structure, which cannot be recovered after the earthquake. The proposed analytical method uses a change in stiffness for handling the geometric nonlinearity and a change in displacement for handling material nonlinearity before solving the equations of motion, thereby separating the effects of geometric nonlinearity and material nonlinearity when computing stiffness forces. This leads directly to integral representations of each energy form. A four-story moment-resisting framed structure is used to demonstrate the feasibility of the proposed analytical method in evaluating the energy response and the transfer among different energy forms throughout the nonlinear response history analysis.

Keywords: Plastic energy, input energy, strain energy, kinetic energy, damping energy

1. Introduction

Structures responding to earthquake shaking can be viewed as an energy transfer process. Earthquake ground motions transfer part of their energy to individual structures as input energy to produce structural vibrations. This input energy induces motion in the structure and its contents, which can generally be characterized as potential energy, kinetic energy, and damping energy. All these energy forms have positive values. While potential energy is related to the structural stiffness and kinetic energy is related to the inertial components, damping energy is associated with energy loss within the structure during its motion. Thus these energy forms have traditionally been investigated as part of the structural responses due to strong ground shaking.

Research on energy dissipation began in the 1980's as an alternative approach for seismic design, when it was recognized that significant cumulative damage can occur in structures without large global displacement responses [1-3] in long-duration earthquake ground motions. However, these studies focused on evaluating the hysteretic energy by calculating the enclosed area in a force-deformation curve of single degree of freedom systems. A numerical procedure was proposed for quantifying different energy forms for low to medium rise structures in the 1990's for linear multi-degree of freedom systems [4], and later an analytical method was developed to consider energy due to inelastic deformation [5]. These studies did not consider the reduction of lateral stiffness by axial load, which can bring considerable error in the calculation of potential energy when this effect becomes prominent.

In this research, a new analytical method of using nonlinear stiffness matrices for both geometric nonlinearity and material nonlinearity is derived to investigate the energy of framed structures responding nonlinearly to earthquake ground motions. In particular, the potential energy that is directly related to the nonlinear stiffness of the structure is investigated. This potential energy consists of three components in a fully nonlinear system: (1) the stored linear elastic strain energy; (2) the energy associated with the geometric nonlinear effects – hereby called "higher-order energy"; and (3) plastic energy dissipated by material nonlinearity of the structure. A four-story moment-resisting steel frame is used to demonstrate the feasibility of the proposed analytical method in evaluating the energy response and the transfer among different energy forms throughout the nonlinear response history analysis.

2. Stiffness Matrices for Geometric Nonlinearity

Nonlinear stiffness matrices for performing energy calculations require an accurate representation of the deflected shape of the member. By subjecting the member to an axial force, the use of stability functions is most appropriate because it is derived based on directly solving for the equilibrium equation that is expressed as a fourth-order differential equation. The theory of using stability functions to analyze moment-resisting framed structures was first developed for elastic members in the 1960's [6-8], but it found limited application because of its complexity in the closed-form solution compared to other methods, such as using the *P*-Δ stiffness approach [9] or the geometric stiffness approach [10]. Even with the advances in computing technology, only one research publication was found in the recent literature on the analysis of framed structures using stability functions [11]. However, when higher accuracy is required, the first-order or second-order approximation of the geometric nonlinearity may not be able to capture the nonlinear behavior accurately. Therefore, stability functions are used in this study because these functions can capture the exact shapes of the displacement profile of the member. A detailed derivation of the stiffness matrices can be found in another publication [12], and it is briefly summarized here with the consideration of yielding and formation of plastic hinge.

2.1 Element Stiffness Matrix

Four degrees of freedom (DOFs) are typically used to describe the lateral displacement (v) and rotation (v') at the two ends of a member in a moment-resisting frame. In addition, two plastic hinge locations (PHLs) for bending at the two ends of the member are used to capture the material nonlinear flexural behavior of the plastic hinges (θ''). This altogether gives 6 movements that are needed to describe the deformation of the member. To

compute the element stiffness matrix $\overline{\mathbf{k}}_i$, each of these 6 movements is displaced independently by one unit as shown in Fig. 1 while subjected to an axial compressive load P. Here, V_{1r}, M_{2r}, V_{3r}, M_{4r}, M_{5r}, and M_{6r} represent the required shear forces and moments at the two ends of the member and the corresponding plastic hinge moments to cause the lateral displacements and rotations in the prescribed pattern, and $r = 1,...,6$ represents the six cases of unit displacement patterns of the member's deflection.
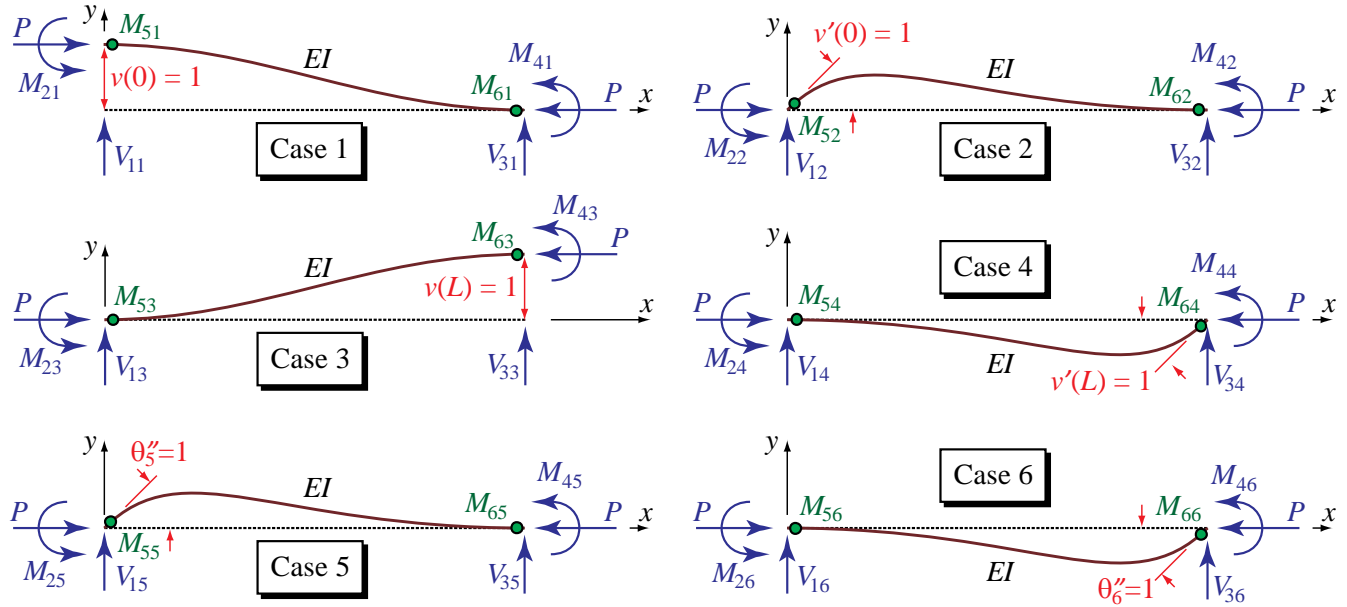

Fig. 1 – Six cases of displacement and plastic rotation patterns and the corresponding fixed-end forces

Using the classical Bernoulli-Euler beam theory with homogeneous and isotropic material properties where the moment is proportional to the curvature and plane sections are assumed to remain plane, the governing equilibrium equation describing the deflected shape of the member can be written as

$$(EIv'')'' + Pv'' = 0 \tag{1}$$

where E is the elastic modulus, I is the moment of inertia, v is the lateral deflection, and each prime represents taking derivatives of the corresponding variable with respect to the x-direction of the member. By assuming EI is constant along the member, the fourth-order ordinary differential equation in Eq. (1) can be solved. Then imposing the boundary conditions as shown in Fig. 1 for each of the four cases, the 6×6 element stiffness matrix $\overline{\mathbf{k}}_i$ can be obtained.

Case 1:

For Case 1 as shown in Fig. 1 (i.e., $r = 1$), imposing the boundary conditions $v(0) = 1$, $v'(0) = 0$, $v(L) = 0$, $v'(L) = 0$, $\theta_5'' = 0$, and $\theta_6'' = 0$, where L is the length of the member, the shears (V) and moments (M) at the two ends based on solving the differential equation in Eq. (1) are calculated as:

$$V_{11} = EIv'''(0) + Pv'(0) = s'EI/L^3 \quad , \quad M_{21} = -EIv''(0) = \overline{s}EI/L^2 \tag{2a}$$

$$V_{31} = -EIv'''(L) - Pv'(L) = -s'EI/L^3 \quad , \quad M_{41} = EIv''(L) = \overline{s}EI/L^2 \tag{2b}$$

$$M_{51} = M_{21} = \overline{s}EI/L^2 \quad , \quad M_{61} = M_{41} = \overline{s}EI/L^2 \tag{2c}$$

where

$$\overline{s} = \frac{\lambda^2(1 - \cos\lambda)}{2 - 2\cos\lambda - \lambda\sin\lambda} \quad , \quad s' = \frac{\lambda^3\sin\lambda}{2 - 2\cos\lambda - \lambda\sin\lambda} \tag{3}$$

and $\lambda = L \times \sqrt{P/EI}$.

Case 2:

For Case 2 as shown in Fig. 1 (i.e., $r = 2$), imposing the boundary conditions $v(0) = 0$, $v'(0) = 1$, $v(L) = 0$, $v'(L) = 0$, $\theta_5'' = 0$, and $\theta_6'' = 0$, the shears and moments at the two ends based on solving the differential equation in Eq. (1) are calculated as:

$$V_{12} = EIv'''(0) + Pv'(0) = \bar{s}EI/L^2 \quad , \quad M_{22} = -EIv''(0) = \hat{s}EI/L \tag{4a}$$

$$V_{32} = -EIv'''(L) - Pv'(L) = -\bar{s}EI/L^2 \quad , \quad M_{42} = EIv''(L) = \hat{s}\hat{c}EI/L \tag{4b}$$

$$M_{52} = M_{22} = \hat{s}EI/L \quad , \quad M_{62} = M_{42} = \hat{s}\hat{c}EI/L \tag{4c}$$

where

$$\hat{s} = \frac{\lambda(\sin\lambda - \lambda\cos\lambda)}{2 - 2\cos\lambda - \lambda\sin\lambda} \quad , \quad \hat{c} = \frac{\lambda - \sin\lambda}{\sin\lambda - \lambda\cos\lambda} \tag{5}$$

Case 3:

For Case 3 as shown in Fig. 1 (i.e., $r = 3$), imposing the boundary conditions $v(0) = 0$, $v'(0) = 0$, $v(L) = 1$, $v'(L) = 0$, $\theta_5'' = 0$, and $\theta_6'' = 0$, the shears and moments at the two ends based on solving the differential equation in Eq. (1) are calculated as:

$$V_{13} = EIv'''(0) + Pv'(0) = -s'EI/L^3 \quad , \quad M_{23} = -EIv''(0) = -\bar{s}EI/L^2 \tag{6a}$$

$$V_{33} = -EIv'''(L) - Pv'(L) = s'EI/L^3 \quad , \quad M_{43} = EIv''(L) = -\bar{s}EI/L^2 \tag{6b}$$

$$M_{53} = M_{23} = -\bar{s}EI/L^2 \quad , \quad M_{63} = M_{43} = -\bar{s}EI/L^2 \tag{6c}$$

Case 4:

For Case 4 as shown in Fig. 1 (i.e., $r = 4$), imposing the boundary conditions $v(0) = 0$, $v'(0) = 0$, $v(L) = 0$, $v'(L) = 1$, $\theta_5'' = 0$, and $\theta_6'' = 0$, the shears and moments at the two ends based on solving the differential equation in Eq. (1) are calculated as:

$$V_{14} = EIv'''(0) + Pv'(0) = \bar{s}EI/L^2 \quad , \quad M_{24} = -EIv''(0) = \hat{s}\hat{c}EI/L \tag{7a}$$

$$V_{34} = -EIv'''(L) - Pv'(L) = -\bar{s}EI/L^2 \quad , \quad M_{44} = EIv''(L) = \hat{s}EI/L \tag{7b}$$

$$M_{54} = M_{24} = \hat{s}\hat{c}EI/L \quad , \quad M_{64} = M_{44} = \hat{s}EI/L \tag{7c}$$

Case 5:

For Case 5 as shown in Fig. 1 (i.e., $r = 5$), imposing the boundary conditions $v(0) = 0$, $v'(0) = 0$, $v(L) = 0$, $v'(L) = 0$, $\theta_5'' = 1$, and $\theta_6'' = 0$, the shears and moments at the two ends based on solving the differential equation in Eq. (1) are calculated as:

$$V_{15} = EIv'''(0) + Pv'(0) = \bar{s}EI/L^2 \quad , \quad M_{25} = -EIv''(0) = \hat{s}EI/L \tag{8a}$$

$$V_{35} = -EIv'''(L) - Pv'(L) = -\bar{s}EI/L^2 \quad , \quad M_{45} = EIv''(L) = \hat{s}\hat{c}EI/L \tag{8b}$$

$$M_{55} = M_{25} = \hat{s}EI/L \quad , \quad M_{65} = M_{45} = \hat{s}\hat{c}EI/L \tag{8c}$$

Case 6:

Finally, for Case 6 as shown in Fig. 1 (i.e., $r = 6$), imposing the boundary conditions $v(0) = 0$, $v'(0) = 0$, $v(L) = 0$, $v'(L) = 0$, $\theta_5'' = 0$, and $\theta_6'' = 1$, the shears and moments at the two ends based on solving the differential equation in Eq. (1) are calculated as:

$$V_{16} = EIv'''(0) + Pv'(0) = \bar{s}EI/L^2 \quad , \quad M_{26} = -EIv''(0) = \hat{s}\hat{c}EI/L \tag{9a}$$

$$V_{36} = -EIv'''(L) - Pv'(L) = -\bar{s}EI/L^2 \quad , \quad M_{46} = EIv''(L) = \hat{s}EI/L \tag{9b}$$

$$M_{56} = M_{26} = \hat{s}\hat{c}EI/L \quad , \quad M_{66} = M_{46} = \hat{s}EI/L \tag{9c}$$

In summary, based on Eqs. (2), (4), (6), (7), (8), and (9) for the above six cases, the element stiffness matrix of the ith member $\bar{\mathbf{k}}_i$ for bending after incorporating two plastic hinges and axial compressive force using stability functions becomes:

$$\bar{\mathbf{k}}_i = \begin{bmatrix} V_{11} & V_{12} & V_{13} & V_{14} & V_{15} & V_{16} \\ M_{21} & M_{22} & M_{23} & M_{24} & M_{25} & M_{26} \\ V_{31} & V_{32} & V_{33} & V_{34} & V_{35} & V_{36} \\ M_{41} & M_{42} & M_{43} & M_{44} & M_{45} & M_{46} \\ M_{51} & M_{52} & M_{53} & M_{54} & M_{55} & M_{56} \\ M_{61} & M_{62} & M_{63} & M_{64} & M_{65} & M_{66} \end{bmatrix} = \frac{EI}{L^3} \begin{bmatrix} s' & \bar{s}L & -s' & \bar{s}L & \bar{s}L & \bar{s}L \\ \bar{s}L & \hat{s}L^2 & -\bar{s}L & \hat{s}\hat{c}L^2 & \hat{s}L^2 & \hat{s}\hat{c}L^2 \\ -s' & -\bar{s}L & s' & -\bar{s}L & -\bar{s}L & -\bar{s}L \\ \bar{s}L & \hat{s}\hat{c}L^2 & -\bar{s}L & \hat{s}L^2 & \hat{s}\hat{c}L^2 & \hat{s}L^2 \\ \bar{s}L & \hat{s}L^2 & -\bar{s}L & \hat{s}\hat{c}L^2 & \hat{s}L^2 & \hat{s}\hat{c}L^2 \\ \bar{s}L & \hat{s}\hat{c}L^2 & -\bar{s}L & \hat{s}L^2 & \hat{s}\hat{c}L^2 & \hat{s}L^2 \end{bmatrix} \begin{matrix} \leftarrow v(0) \\ \leftarrow v'(0) \\ \leftarrow v(L) \\ \leftarrow v'(L) \\ \leftarrow -\theta_5'' \\ \leftarrow -\theta_6'' \end{matrix} \tag{10}$$

2.2 Global Stiffness Matrices

The element stiffness matrix presented in Eq. (10) needs to be assembled into the global stiffness matrix. This assembly procedure can be simplified by partitioning the element stiffness matrix in Eq. (10) as follows.

$$\bar{\mathbf{k}}_i = \begin{bmatrix} \mathbf{k}_i & \mathbf{k}_i' \\ \mathbf{k}_i'^T & \mathbf{k}_i'' \end{bmatrix} \tag{11}$$

where

$$\mathbf{k}_i = \frac{EI}{L^3} \begin{bmatrix} s' & \bar{s}L & -s' & \bar{s}L \\ \bar{s}L & \hat{s}L^2 & -\bar{s}L & \hat{s}\hat{c}L^2 \\ -s' & -\bar{s}L & s' & -\bar{s}L \\ \bar{s}L & \hat{s}\hat{c}L^2 & -\bar{s}L & \hat{s}L^2 \end{bmatrix} \quad , \quad \mathbf{k}_i' = \frac{EI}{L^2} \begin{bmatrix} \bar{s} & \bar{s} \\ \hat{s}L & \hat{s}\hat{c}L \\ -\bar{s} & -\bar{s} \\ \hat{s}\hat{c}L & \hat{s}L \end{bmatrix} \quad , \quad \mathbf{k}_i'' = \frac{EI}{L} \begin{bmatrix} \hat{s} & \hat{s}\hat{c} \\ \hat{s}\hat{c} & \hat{s} \end{bmatrix} \tag{12}$$

From the sub-matrices partitioned according in Eq. (12), the assembly into the global stiffness matrices $\mathbf{K}(t)$, $\mathbf{K}'(t)$, and $\mathbf{K}''(t)$ follows a straightforward procedure. Here, the global stiffness matrices are functions of time, since the axial compressive load P is a function of time in a dynamic analysis. A number of textbooks have discussed this procedure in great detail [13]. Consider a framed structure having a total of n DOFs and m PHLs, the global stiffness matrices can be obtained by this assembly procedure and are often written in the form:

$$\mathbf{K}(t) = \begin{bmatrix} \textit{Assembly of } \mathbf{k}_i \end{bmatrix}_{n \times n} \quad , \quad \mathbf{K}'(t) = \begin{bmatrix} \textit{Assembly of } \mathbf{k}_i' \end{bmatrix}_{n \times m} \quad , \quad \mathbf{K}''(t) = \begin{bmatrix} \textit{Assembly of } \mathbf{k}_i'' \end{bmatrix}_{m \times m} \tag{13}$$

3. Inelastic Displacement for Material Nonlinearity

The detailed derivation on the use of inelastic displacement for analyzing structures with material nonlinearity has been published [14] and it is briefly summarized here. Consider a moment-resisting framed structure having

a total of n DOFs and m PHLs. Let the $n \times 1$ total displacement $\mathbf{x}(t)$ at each DOF be represented as the summation of the $n \times 1$ elastic displacement $\mathbf{x}'(t)$ and the $n \times 1$ inelastic displacement $\mathbf{x}''(t)$:

$$\mathbf{x}(t) = \mathbf{x}'(t) + \mathbf{x}''(t) \tag{14}$$

Similarly, let the $m \times 1$ total moment $\mathbf{m}(t)$ at the PHLs of a moment-resisting frame be separated into the $m \times 1$ elastic moment $\mathbf{m}'(t)$ and the $m \times 1$ inelastic moment $\mathbf{m}''(t)$:

$$\mathbf{m}(t) = \mathbf{m}'(t) + \mathbf{m}''(t) \tag{15}$$

The displacements in Eq. (14) and the moments in Eq. (15) are related by the equations:

$$\mathbf{m}'(t) = \mathbf{K}'(t)^T \mathbf{x}'(t) \quad , \quad \mathbf{m}''(t) = -\left[\mathbf{K}''(t) - \mathbf{K}'(t)^T \mathbf{K}(t)^{-1}\mathbf{K}'(t)\right]\mathbf{\Theta}''(t) \tag{16}$$

where $\mathbf{\Theta}''(t)$ is the $m \times 1$ plastic rotation at each PHL, and $\mathbf{K}(t)$, $\mathbf{K}'(t)$, and $\mathbf{K}''(t)$ are calculated in Eq. (13). The relationship between the plastic rotation $\mathbf{\Theta}''(t)$ and inelastic displacement $\mathbf{x}''(t)$ is:

$$\mathbf{x}''(t) = \mathbf{K}(t)^{-1}\mathbf{K}'(t)\mathbf{\Theta}''(t) \tag{17}$$

Substituting both equations in Eq. (16) into Eq. (15) and making use of Eqs. (14) and (17), then rearranging the terms gives the governing equation for calculating the plastic hinge responses for any given total displacement pattern:

$$\mathbf{m}(t) + \mathbf{K}''\mathbf{\Theta}''(t) = \mathbf{K}'^T \mathbf{x}(t) \tag{18}$$

4. Dynamic Equilibrium Equation of Motion

For a moment-resisting framed structure modeled as an n DOF system and subjected to earthquake ground motions, the dynamic equilibrium equation of motion can be written as

$$\mathbf{M}\ddot{\mathbf{x}}(t) + \mathbf{C}\dot{\mathbf{x}}(t) + \mathbf{K}(t)\mathbf{x}'(t) = -\mathbf{M}\ddot{\mathbf{g}}(t) - \mathbf{F}_a(t) \tag{19}$$

where $\mathbf{M}$ is the $n \times n$ mass matrix, $\mathbf{C}$ is the $n \times n$ damping matrix, $\dot{\mathbf{x}}(t)$ is the $n \times 1$ velocity vector, $\ddot{\mathbf{x}}(t)$ is the $n \times 1$ acceleration vector, $\mathbf{K}(t)$ is the time-varying $n \times n$ stiffness matrix derived in Eq. (13) while subjected to time-varying column axial compressive load $P(t)$, $\ddot{\mathbf{g}}(t)$ is the $n \times 1$ earthquake ground acceleration vector corresponding to the effect of ground motion at each DOF, and $\mathbf{F}_a(t)$ is the $n \times 1$ vector of additional forces imposed on the structure due to geometric nonlinearity accounting for all the gravity columns in the structure (mainly the *P-Δ* effect). This geometric nonlinearity can often be modeled using a leaning column (or sometimes called a *P-Δ* column) in a two-dimensional analysis but may require more detailed modeling of all gravity columns in a three-dimensional analysis to capture the response due to torsional irregularity of the structure. In a two-dimensional analysis, the relationship between this lateral force $\mathbf{F}_a(t)$ and the lateral displacement can be written as follows:

$$\mathbf{F}_a(t) = \mathbf{K}_a \mathbf{x}(t) \tag{20}$$

where $\mathbf{K}_a$ is an $n \times n$ stiffness matrix that is a function of the gravity loads on the leaning column and the corresponding story height, but it is not a function of time. For two-dimensional frames with horizontal DOFs only, this $\mathbf{K}_a$ matrix often takes the form:

$$\mathbf{K}_a = \begin{bmatrix} -Q_1/h_1 - Q_2/h_2 & Q_2/h_2 & 0 & \cdots & 0 \\ Q_2/h_2 & -Q_2/h_2 - Q_3/h_3 & \ddots & \ddots & \vdots \\ 0 & \ddots & \ddots & Q_{n-1}/h_{n-1} & 0 \\ \vdots & \ddots & Q_{n-1}/h_{n-1} & -Q_{n-1}/h_{n-1} - Q_n/h_n & Q_n/h_n \\ 0 & \cdots & 0 & Q_n/h_n & -Q_n/h_n \end{bmatrix} \tag{21}$$

where Q_i is the total axial force due to gravity loads acting on the leaning column of the ith floor, and h_i is the story height of the ith floor. Now substituting Eq. (20) into Eq. (19) and rearranging terms gives

$$\mathbf{M}\ddot{\mathbf{x}}(t) + \mathbf{C}\dot{\mathbf{x}}(t) + \mathbf{K}(t)\mathbf{x}'(t) + \mathbf{K}_a\mathbf{x}(t) = -\mathbf{M}\ddot{\mathbf{g}}(t) \tag{22}$$

Since $\ddot{\mathbf{y}}(t) = \ddot{\mathbf{x}}(t) + \ddot{\mathbf{g}}(t)$ where $\ddot{\mathbf{y}}(t)$ is the $n \times 1$ absolute acceleration vector, substituting this equation into Eq. (22) gives the governing equation of motion for energy balance:

$$\mathbf{M}\ddot{\mathbf{y}}(t) + \mathbf{C}\dot{\mathbf{x}}(t) + \mathbf{K}(t)\mathbf{x}'(t) + \mathbf{K}_a\mathbf{x}(t) = \mathbf{0} \tag{23}$$

While the lateral force $\mathbf{F}_a(t) = \mathbf{K}_a\mathbf{x}(t)$ in Eq. (23) takes care of the nonlinear geometric effects from all the gravity columns in the structure, the stiffness matrix $\mathbf{K}(t)$ in Eq. (23) considers both large P-Δ and small P-δ effects of geometric nonlinearity on the moment-resisting frame itself. Let this time-dependent global stiffness matrix $\mathbf{K}(t)$ be represented in the form:

$$\mathbf{K}(t) = \mathbf{K}_L + \mathbf{K}_G(t) \tag{24}$$

where $\mathbf{K}_L$ denotes the linearized elastic stiffness of the frame due to the gravity loads on the frame only, and $\mathbf{K}_G(t)$ denotes the change in the geometric stiffness due to the change in axial load on the frame during the dynamic loading. Since the $\mathbf{K}_L$ matrix is computed by using the gravity loads on the columns of the frame (which means $\mathbf{K}_L = \mathbf{K}(t_0) = \mathbf{K}(0)$, i.e., the stiffness matrix computed at time step 0) only, it is not a function of time and therefore remains as a constant throughout the dynamic analysis.

5. Energy Balance

Seismic energy evaluation begins with Eq. (23). Integrating this equation over the path of displacement response gives

$$\int_0^t \ddot{\mathbf{y}}(t)^T \mathbf{M}d\mathbf{x} + \int_0^t \dot{\mathbf{x}}(t)^T \mathbf{C}d\mathbf{x} + \int_0^t \mathbf{x}'(t)^T \mathbf{K}(t)d\mathbf{x} + \int_0^t \mathbf{x}(t)^T \mathbf{K}_a d\mathbf{x} = 0 \tag{25}$$

Note that $d\mathbf{x}(t) = d\mathbf{y}(t) - d\mathbf{g}(t)$, where $\mathbf{y}(t)$ is the $n \times 1$ absolute displacement vector and $\mathbf{g}(t)$ is the $n \times 1$ earthquake ground displacement vector. Now substituting this equation into the first integral of Eq. (25) gives

$$\int_0^t \ddot{\mathbf{y}}(t)^T \mathbf{M}d\mathbf{y} + \int_0^t \dot{\mathbf{x}}(t)^T \mathbf{C}d\mathbf{x} + \int_0^t \mathbf{x}'(t)^T \mathbf{K}(t)d\mathbf{x} + \int_0^t \mathbf{x}(t)^T \mathbf{K}_a d\mathbf{x} = \int_0^t \ddot{\mathbf{y}}(t)^T \mathbf{M}d\mathbf{g} \tag{26}$$

In addition, Eq. (14) can be expressed in incremental form as $d\mathbf{x}(t) = d\mathbf{x}'(t) + d\mathbf{x}''(t)$. Substituting this equation into the third integral of Eq. (26) gives

$$\int_0^t \ddot{\mathbf{y}}(t)^T \mathbf{M}d\mathbf{y} + \int_0^t \dot{\mathbf{x}}(t)^T \mathbf{C}d\mathbf{x} + \int_0^t \mathbf{x}'(t)^T \mathbf{K}(t)d\mathbf{x}' + \int_0^t \mathbf{x}(t)^T \mathbf{K}_a d\mathbf{x} + \int_0^t \mathbf{x}'(t)^T \mathbf{K}(t)d\mathbf{x}'' = \int_0^t \ddot{\mathbf{y}}(t)^T \mathbf{M}d\mathbf{g} \tag{27}$$

Each integral in Eq. (27) is considered separately in the following sub-sections.

5.1 Kinetic Energy (*KE*)

The first integral on the left hand side of Eq. (27) represents the absolute kinetic energy (*KE*) and can be evaluated using absolute velocity of the structure as:

$$KE(t_k) = \int_0^{t_k} \ddot{\mathbf{y}}(t)^T \mathbf{M}d\mathbf{y} = \frac{1}{2}\dot{\mathbf{y}}(t_k)^T \mathbf{M}\dot{\mathbf{y}}(t_k) - \frac{1}{2}\dot{\mathbf{y}}(0)^T \mathbf{M}\dot{\mathbf{y}}(0) = \frac{1}{2}\dot{\mathbf{y}}_k^T \mathbf{M}\dot{\mathbf{y}}_k \tag{28}$$

where $\dot{\mathbf{y}}(t)$ is the $n \times 1$ absolute velocity vector, $\dot{\mathbf{y}}_k$ represents the discretized form of $\dot{\mathbf{y}}(t_k)$, and t_k represents the kth time step at which the energy value is calculated. The structure is assumed to be at rest when the earthquake begins, and therefore $\dot{\mathbf{y}}(0) = \mathbf{0}$. Due to the squaring of the absolute velocity vector in Eq. (28) and a positive definite $\mathbf{M}$ matrix, the kinetic energy is always positive.

5.2   Damping Energy (*DE*)

The second integral on the left hand side of Eq. (27) represents the damping energy (*DE*), which is the energy dissipated via viscous damping mechanism within the structure. The integrand is always positive, and therefore damping energy always accumulates over time. In terms of numerical simulation, the integral can be numerically approximated by evaluating the area underneath the curve using the trapezoidal rule:

$$DE(t_k) = \int_0^{t_k} \dot{\mathbf{x}}(t)^T \mathbf{C} d\mathbf{x} = \sum_{k=1}^{t_k} \frac{1}{2}\left(\dot{\mathbf{x}}_{k-1}^T + \dot{\mathbf{x}}_k^T\right)\mathbf{C}\left(\mathbf{x}_k - \mathbf{x}_{k-1}\right)$$ (29)

where $\mathbf{x}_k$ and $\dot{\mathbf{x}}_k$ represent the discretized forms of $\mathbf{x}(t_k)$ and $\dot{\mathbf{x}}(t_k)$, respectively.

5.3   Strain Energy (*SE*)

The third integral on the left hand side of Eq. (27) represents strain energy (*SE*) of the moment-resisting frame. Since the stiffness matrix $\mathbf{K}(t)$ is time-varying, obtaining a closed form solution to the integral is not possible. However, an assumption can be made by setting the $\mathbf{K}_G(t)$ matrix in Eq. (24) to zero, indicating that the overall gravity loads on the frame as a whole remains constant even though the axial forces in individual columns may vary. Based on this assumption, Eq. (24) becomes $\mathbf{K}(t) = \mathbf{K}_L$, and the strain energy of the moment-resisting frame is calculated as

$$SE(t_k) = \int_0^{t_k} \mathbf{x}'(t)^T \mathbf{K}(t) d\mathbf{x}' = \int_0^{t_k} \mathbf{x}'(t)^T \mathbf{K}_L d\mathbf{x}' = \frac{1}{2}\mathbf{x}'(t_k)^T \mathbf{K}_L \mathbf{x}'(t_k) - \frac{1}{2}\mathbf{x}'(0)^T \mathbf{K}_L \mathbf{x}'(0) = \frac{1}{2}\mathbf{x}_k'^T \mathbf{K}_L \mathbf{x}_k'$$ (30)

where $\mathbf{x}_k'$ represents the discretized form of $\mathbf{x}'(t_k)$. The structure is again assumed to be at rest when the earthquake begins, and therefore $\mathbf{x}'(0) = \mathbf{0}$. Due to the squaring of the elastic displacement vector in Eq. (30) and a positive definite $\mathbf{K}_L$ matrix, the strain energy is always positive.

5.4   Higher-order Energy (*HE*)

The fourth integral on the left hand side of Eq. (27) represents higher-order energy (*HE*) due to gravity loads on the structure itself. It is of higher-order because the energy comes from the large *P*-Δ effect on the gravity columns and is calculated as follows:

$$HE(t_k) = \int_0^{t_k} \mathbf{x}(t)^T \mathbf{K}_a d\mathbf{x} = \frac{1}{2}\mathbf{x}(t_k)^T \mathbf{K}_a \mathbf{x}(t_k) - \frac{1}{2}\mathbf{x}(0)^T \mathbf{K}_a \mathbf{x}(0) = \frac{1}{2}\mathbf{x}_k^T \mathbf{K}_a \mathbf{x}_k$$ (31)

where the structure is again assumed to be at rest when the earthquake begins, and therefore $\mathbf{x}(0) = \mathbf{0}$. Due to the squaring of the total displacement vector in Eq. (31) and a negative definite $\mathbf{K}_a$ matrix as shown in Eq. (21), the higher-order energy is always negative and varies with time.

5.5   Plastic Energy (*PE*)

The fifth integral on the left hand side of Eq. (27), which is associated with inelastic displacements, represents the plastic energy (*PE*) dissipated by the permanent deformations of the structure. Rewriting Eqs. (16) and (17) in the forms:

$$\mathbf{K}(t)d\mathbf{x}'' = \mathbf{K}'(t)d\mathbf{\Theta}'' \quad , \quad \mathbf{x}'(t)^T \mathbf{K}'(t) = \mathbf{m}'(t)^T$$ (32)

Then substituting Eq. (32) into the fifth integral of Eq. (27) gives

$$PE(t_k) = \int_0^{t_k} \mathbf{x}'(t)^T \mathbf{K}(t) d\mathbf{x}'' = \int_0^{t_k} \mathbf{x}'(t)^T \mathbf{K}'(t) d\mathbf{\Theta}'' = \int_0^{t_k} \mathbf{m}'(t)^T d\mathbf{\Theta}'' = \sum_{i=1}^m \int_0^{t_k} m_i'(t) d\theta_i'' = \sum_{i=1}^m PE_i(t_k)$$ (33)

where PE_i represents the plastic energy dissipation at the ith plastic hinge, $i = 1,...,m$. Through this analytical derivation, it is shown in Eq. (33) that the overall plastic energy dissipation is exactly equal to the sum of plastic energy dissipation in all the plastic hinges.

The term PE_i in Eq. (33) can be numerically approximated by evaluating the area underneath the curve using the trapezoidal rule:

$$PE_i = \int_0^{t_k} m_i'(t)d\theta_i'' = \sum_{k=1}^{t_k} \frac{1}{2}\left(m_{i,k-1}' + m_{i,k}'\right)\left(\theta_{i,k}'' - \theta_{i,k-1}''\right) \tag{34}$$

where $m_{i,k}'$ and $\theta_{i,k}''$ represent the discretized forms of $m_i'(t_k)$ and $\theta_i''(t_k)$, respectively.

Note that PE_i is computed by integrating the product of elastic moment m_i' and the change in plastic rotation $d\theta_i''$. A positive change in plastic rotation is always caused by a positive moment, and a negative change in plastic rotation is always caused by a negative moment. Therefore, PE_i is always positive and accumulates over time.

5.6 Input Energy (*IE*)

Finally, the integral on the right side of Eq. (27) represents the absolute input energy (*IE*) due to the earthquake ground motion, and this integral can be numerically approximated by evaluating the area underneath the curve using the trapezoidal rule:

$$IE(t_k) = \int_0^{t_k} \ddot{\mathbf{y}}(t)^T \mathbf{M} d\mathbf{g} = \sum_{k=1}^{t_k} \frac{1}{2}\left(\ddot{\mathbf{y}}_{k-1}^T + \ddot{\mathbf{y}}_k^T\right)\mathbf{M}\left(\mathbf{g}_k - \mathbf{g}_{k-1}\right) \tag{35}$$

where $\ddot{\mathbf{y}}_k$ and $\mathbf{g}_k$ represent the discretized forms of $\ddot{\mathbf{y}}(t_k)$ and $\mathbf{g}(t_k)$, respectively.

In summary, substituting Eqs. (28), (29), (30), (31), (33), and (35) into Eq. (27), the energy balance equation becomes

$$KE + DE + SE + HE + PE = IE \tag{36}$$

6. Numerical Simulation of a 4-story Moment-Resisting Frame

To illustrate the use of Eq. (36) in calculating the energy dissipation of moment-resisting frames, consider the four-story frame shown in Fig. 2(a). This frame contains 36 DOFs (i.e., $n = 36$). and 56 PHLs (i.e., $m = 56$). Assume a mass of 72,670 kg is used on each floor, and a gravity load of 431 kN is applied on each exterior column member and 632 kN is applied on each interior column member as shown in Fig. 2(b). In addition, a leaning column is used in the model to account for all of the gravity loads from other parts of the structure as shown in Fig. 2(b). The gravity loads on the leaning column is assumed to be 2,018 kN per floor. A 2% damping is assumed in all four modes of vibration.
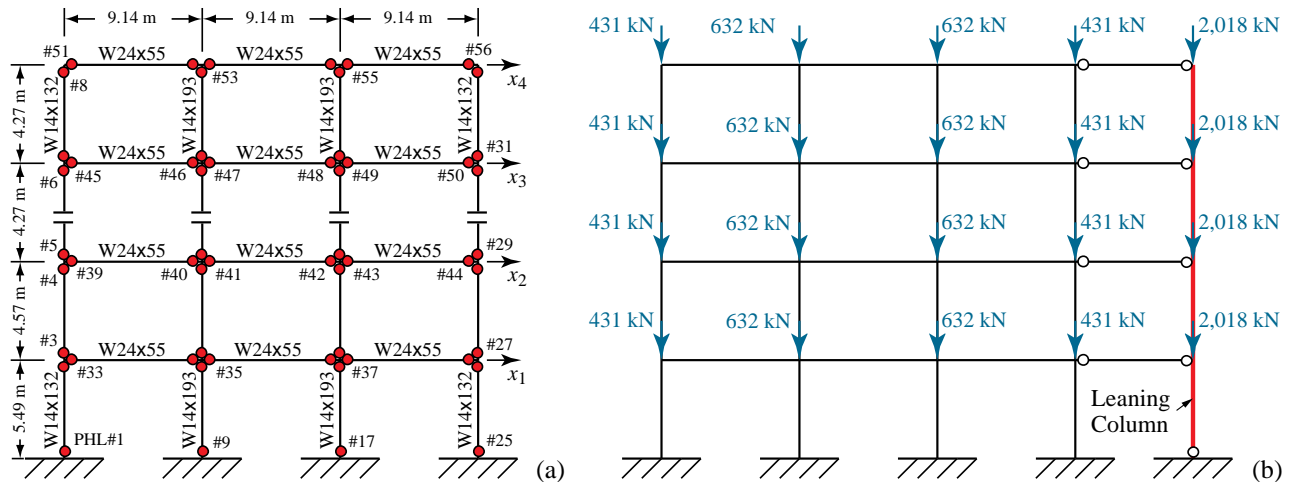

Fig. 2 – Four-story moment-resisting steel frame and corresponding gravity loads

Assume the yield stress of the member is 345 MPa and all 56 plastic hinges exhibit elastic-plastic behavior. By subjecting the steel frame to the 1995 Kobe earthquake ground acceleration shown in Fig. 3, the energy responses are summarized in Fig. 4, where the case "without axial force" represents the approach used in previous research [5] and the case "with axial force" represents the present approach with geometric nonlinearity due to axial force considered in the stiffness formulation. The results confirm that KE and SE are always positive, DE and PE are accumulative and never decreasing, and HE is always negative. The magnitude of HE is smaller than that of DE and PE, and therefore IE tends to follow an increasing trend. One interesting point to note is that HE has a larger magnitude than SE after 10 s, indicating that higher-order energy builds up quickly when permanent deformation occurs in the structure due to yielding.
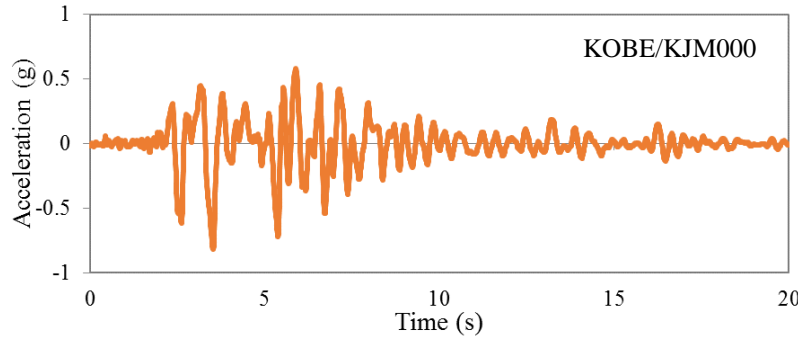

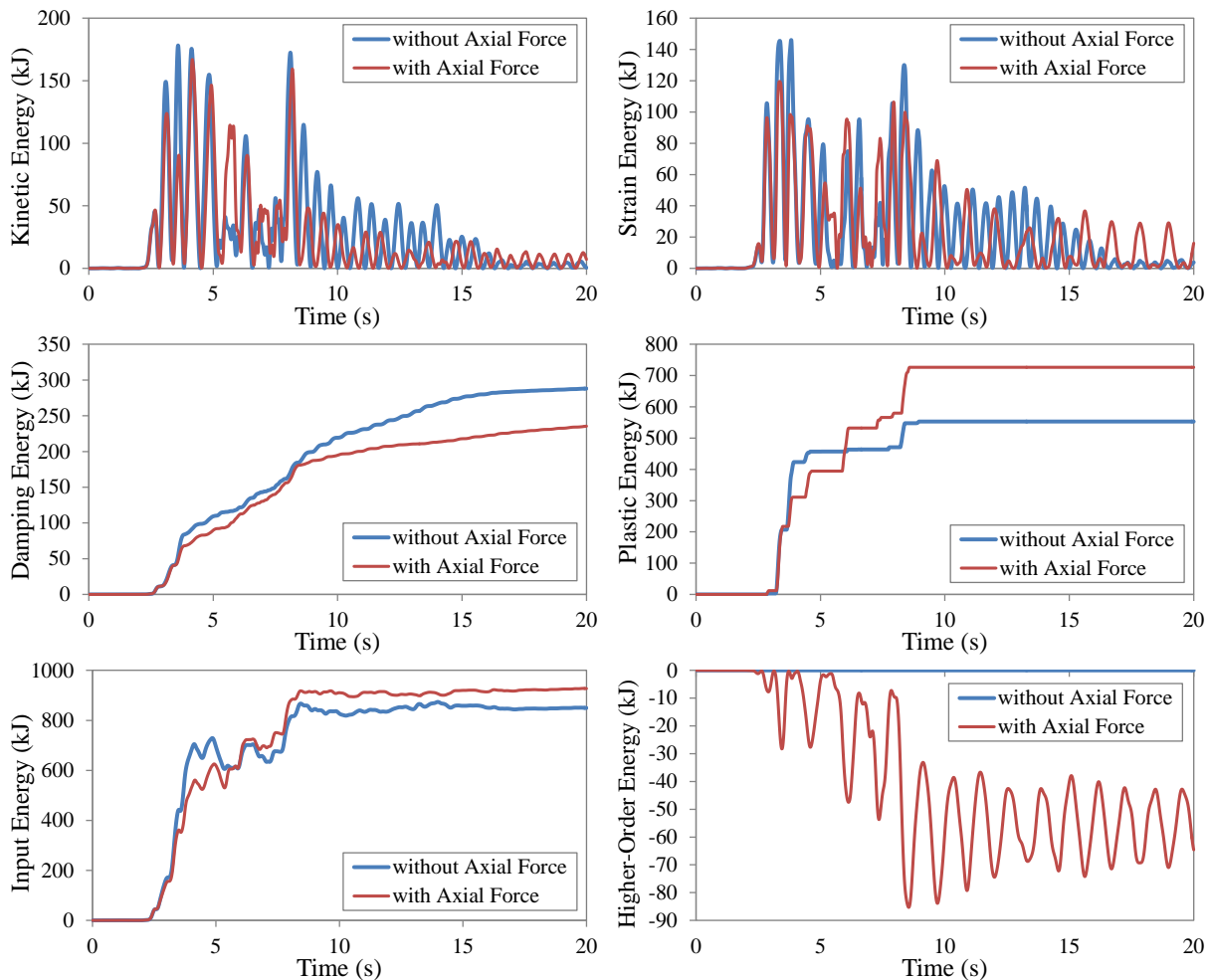Fig. 3 – Recorded 1995 Kobe earthquake ground motion at Kajima station Component 000

Fig. 4 – Energy response of the 4-story framed structure with geometric nonlinearity due to Kobe earthquake

10

In terms of energy dissipation, it can be seen from Fig. 4 that both *KE* and *SE* diminish slowly as the earthquake subsides, and the energy components responsible for dissipating the *IE* due to the earthquake are *DE* and *PE*. As shown in Fig. 4, the input energy to the frame is approximately the same for the cases with and without axial force modeled for geometric nonlinearity. However, when geometric nonlinearity is considered, larger *PE* dissipation is needed with smaller *DE* dissipation, verifying that geometric nonlinearity causes more damage to the structure.

In terms of plastic energy dissipation at individual plastic hinges, Fig. 5(a) shows the maximum plastic energy at each plastic hinge, i.e., PE_i. Since plastic energy accumulates over time, the maximum plastic energy always occurs at the end of the earthquake duration. In addition, summing the plastic energy values at all the plastic hinges in Fig. 5(a) gives the total plastic energy dissipation *PE* in Fig. 4, confirming Eq. (33) is correct. Finally, Fig. 5(b) shows the relative proportion of each energy component of those shown in Fig.5(a) for the frame with geometric nonlinearity that makes up the input energy. It can be seen from this figure that *PE* is at least three times larger than *DE*, illustrating that damage to the plastic hinges is the major source of energy dissipation for the four-story frame due to the Kobe earthquake ground motion.
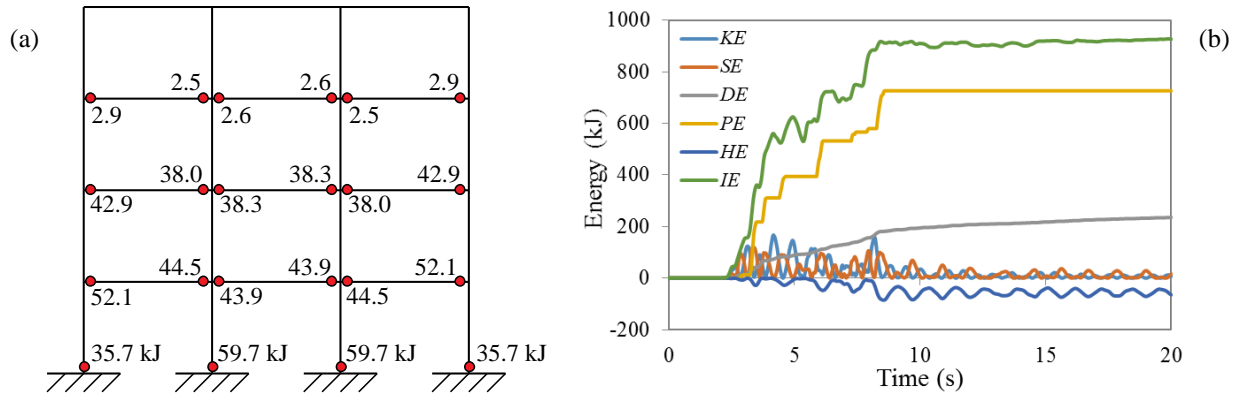

Fig. 5 – Energy response of structure with geometric nonlinearity: (a) Plastic energy dissipation at individual plastic hinges and (b) portions of individual energies making up the input energy

By including the axial force in the formulation, different forms of potential energy can now be captured and balanced. More importantly, based on the above analytical derivation and numerical example, a computational tool based on small displacement approach is now available to capture the dissipated plastic energy in the inelastic components of the structure that considers both geometric and material nonlinearities. In addition, the analytical derivation proves that the sum of dissipation plastic energy at each inelastic component equals the overall plastic energy dissipation, which is an energy form of the energy balance equation. Because of the accumulative nature of plastic energy, it can be used in a wide range of applications. These potential applications include:

- Assessment of structural damage via the comparison of plastic energy demand with the corresponding plastic energy capacity of members.

- Evaluation of residual capacity of the structure after suffering damage during an earthquake event.

- Development of assessment metrics for structural performance.

7. Conclusion

An analytical theory and the corresponding computational method for evaluating the seismic energy in structures are presented based on the use of stability functions in the formulation of the stiffness matrix. The proposed method successfully separates the coupling effect of material nonlinearity and geometric nonlinearity by using inelastic displacement. By expressing the input energy as the sum of kinetic energy, damping energy, strain

energy, higher-order energy, and plastic energy, as summarized by Eq. (36), the energy representation of the structural response due to earthquake ground motion is complete. For potential energy in particular,

- Strain energy (*SE*) represents the linear elastic portion of the structural response that is recoverable;

- Higher-order energy (*HE*) represents the addition or subtraction of energy from the overall structural response due to geometric nonlinear effects; and

- Plastic energy (*PE*) represents the dissipation of energy and reduction of structural response due to material nonlinearity.

Careful attention should be paid to the difference between *HE* and *PE*, even though both represent the nonlinear energy response of the structure. While *PE* represents damage in the structure resulting from inelastic deformation, *HE* represents the stored energy due the higher-order effect of gravity loads acting on the gravity columns, which contains both elastic displacement response and inelastic displacement response due to yielding of the structure. Therefore, the coupling effect between geometric nonlinearity and material nonlinearity, which is often found in the calculation of structural displacement responses, occurs in the energy calculation also.

8. Disclaimer

No formal investigation to evaluate potential sources of uncertainty or error, or whether multiple sources of error are correlated, was included in this study. The question of uncertainties in the analytical models, solution algorithms, material properties and as-built final dimensions and positions of members versus design configurations employed in analysis are beyond the scope of the work reported here.

9. References

[1] Tembulkar J, Nau JM (1987): Inelastic modeling and seismic energy dissipation. *Journal of Structural Engineering ASCE*, **113** (6), 1373-1377.

[2] Fajfar P, Vidic T, Fischinger M (1989): Seismic demand in medium-period and long-period structures. *Earthquake Engineering and Structural Dynamics*, **18** (8), 1133-1144.

[3] Fajfar P (1992): Equivalent ductility factors, taking into account low-cycle fatigue. *Earthquake Engineering and Structural Dynamics*, **21** (10), 837-848.

[4] Uang CM, Bertero VV (1990): Evaluation of seismic energy in structures. *Earthquake Engineering and Structural Dynamics*, **19** (1), 77-90.

[5] Wong KKF, Yang R (2002): Earthquake response and energy evaluation of inelastic structures. *Journal of Engineering Mechanics ASCE*, **128** (3), 308-317.

[6] Timoshenko SP, Gere JM (1961): *Theory of Elastic Stability, 2nd Edition*, McGraw Hill, NY, USA.

[7] Horne MZ, Merchant W (1965): *The Stability of Frames*, Pergamon Press, NY, USA.

[8] Bazant ZP, Cedolin L (2003): *Stability of Structures*, Dover Publication, NY, USA.

[9] Powell GH (2010): *Modeling for Structural Analysis: Behavior and Basics*, Computers and Structures Inc., CA, USA.

[10] Wilson E (2010): *Static and Dynamic Analysis of Structures: A Physical Approach with Emphasis on Earthquake Engineering, 4th Edition*, Computer and Structures Inc., CA, USA.

[11] Park JW, Kim SE (2008): Nonlinear inelastic analysis of steel-concrete composite beam-columns using the stability functions. *Structural Engineering and Mechanics*, **30** 6, 763-785.

[12] Li G, Wong KKF (2014): *Theory of Nonlinear Structural Analysis: The Force Analogy Method for Earthquake Engineering*, John Wiley and Sons, Singapore.

[13] Hibbeler RC (2012): *Structural Analysis, 8th Edition*, Prentice Hall, NJ, USA.

[14] Wong KKF, Yang R (1999): Inelastic dynamic response of structures using force analogy method. *Journal of Engineering Mechanics ASCE*, **125** (10), 1190-1199.